Geocarto International

ISSN: (Print) (Online) Journal homepage: https://www.tandfonline.com/loi/tgei20

Seasonal Ice Flow Velocity variations of Polar Record Glacier, East Antarctica during 2016-2019 using Sentinel-1 data

Kiledar Singh Tomar, Sheetal Kumari & Alvarinho J. Luis

To cite this article: Kiledar Singh Tomar, Sheetal Kumari & Alvarinho J. Luis (2021): Seasonal Ice Flow Velocity variations of Polar Record Glacier, East Antarctica during 2016-2019 using Sentinel-1 data, Geocarto International, DOI: 10.1080/10106049.2021.1892211

To link to this article: https://doi.org/10.1080/10106049.2021.1892211

Accepted author version posted online: 25 Feb 2021.

Seasonal Ice Flow Velocity variations of Polar Record Glacier, East Antarctica during 2016-2019 using Sentinel-1 data

Kiledar Singh Tomar[1], Sheetal Kumari[2] and Alvarinho J. Luis[1]

[1]ESSO-National Centre for Polar and Ocean Research, Ministry of Earth Sciences, Headland Sada, Goa, India.

[2]Central University of Jharkhand, Department of Geoinformatics, Ranchi, India

Corresponding author: Kiledar Singh Tomar, ESSO- National Centre for Polar and Ocean Research, Goa, India, kdsingh108@hotmail.com; cc: alvluis@gmail.com

Remote sensing-based investigation of ice flow dynamics of Polar Record glacier (PRG) during December–April of 2016-2019 has been conducted in this work. Using offset tracking method on the Sentinel-1 Synthetic Aperture Radar (SAR) images, we estimated the glacier ice flow velocity. Ice flow velocity near the glacier terminus indicated higher velocity during January and subsequently showed lower values in December during 2016-2019. The maximum and minimum velocity of the glacier was found to be ~2.54 and 0.03 m/d for 2016-2017, ~2.49 and 0.03 m/d for 2017-2018, and ~2.47 and 0.03 m/d for 2018-2019. Results indicate that the maximum velocity occurred at the terminus of the glacier and minimum flow was detected on the ice sheet portion of the glacier. The average ice front position receded from ~900 m in 2016-2017 to ~650 m in 2017-2018 to ~200 m in 2018-2019. However, a slowdown near the glacier terminus is observed for the period 2018-2019, which led to the glacier advance by 25 km^2 from 877 km^2 to 905 km^2. The enhanced velocity at the terminus in the early winter (March and April) was attributed to ice-free water surrounding the PRG terminus which eliminated the buttressing effect.

Keywords: Polar Record Glacier, Sentinel-1 SAR data, offset tracking, flow velocity, East Antarctica

1. Introduction

The 14 million km^2 Antarctic ice sheet consists of the Antarctic Peninsula Ice sheet, West Antarctic Ice Sheet, and the East Antarctic Ice Sheet (EAIS) (Rémy and Frezzotti 2006). Most of the coastline of the Antarctic continent is composed of grounded or floating ice and ice shelves (Bindschadler et al. 2011). The glaciers that are marine-terminating consist of tidewater glaciers, ice-shelf tributary glaciers, or grounded outlet glaciers. The EAIS is considered as the largest reserve of fresh water present on Earth, which, if melted, is capable of raising the sea level by ~50 m (Stearns 2011). From the past many years, the status of EAIS remains uncertain, concerning whether it is gaining or losing mass (Hanna et al. 2013). Due to global warming, the increased flow of major glaciers, as well as ice streams of Antarctica, has been one of the main contributors to ice-mass loss from ice-shelf (Hanna et al. 2013). These large ice streams and outlet glaciers primarily facilitate the ice loss through ice conveyance from the inner region of East Antarctica to the ocean (Eric Rignot 2002; Stearns 2011; E. Rignot et al. 2013).

The outlet glaciers which undergo a change in their speed over a time span, which demonstrate their dynamic response to the changes in climate (Scambos et al. 2004; Stearns, Smith, and Hamilton 2008). Variations in the velocity of large outlet glaciers in Antarctica are crucial for understanding mass balance of ice-sheets and sea-level rise (Stearns, Smith, and Hamilton 2008). However, the abrupt changes cause in outlet glacier flow speed are complex (Stearns, Smith, and Hamilton 2008). It has been pointed out that the summer-time melting and surface meltwater are not the only reasons for changes in the dynamics of outlet glacier because East Antarctica is too cold (Stearns, Smith, and Hamilton 2008). In view of this, the Polar Record glacier (PRG) needs attention as it is one of the largest outlet glacier in East Antarctica.

The glacier surface velocity is one of the significant processes involved in understanding the glacier dynamics. It also serves as an alternative to other glacier features such as mass balance and long-term glacier-area-change information to understand the behaviour of glaciers (Sahu et al., 2019). For better monitoring of glacier dynamics and its response to climate change, spatial and temporal analysis of glacier surface velocity is of paramount importance. Remote Sensing techniques are viable for glacier like PRG which is full of crevasses to provide detail and timely observation. Though, the ground truth of the glacier velocity is possible to be measured at few locations, the interpolation-based remote sensing measurements provide estimates over a wide area of the glacier (Raup et al. 2014). Earlier studies addressed the dynamics of this glacier utilizing remote sensing techniques. Liang *et al.* (2019) reported ice flow variations at the PRG from 2005 to 2015 which showed an overall 15% speedup of PRG with seasonal variations. (Liu, Niu, and Yang 2018) derived surface velocity through a novel rotation-invariant feature-tracking technique applied to Landsat-7 enhanced thematic mapper plus images for the 2005 to 2015 period and reported a maximum ice velocity of the frontal margin of ~900 m/a and 1000 m/a at the frontal iceberg region. They also found no significant trend in velocity. (Zhou et al. 2014) reported ice velocity changes at seasonal and interannual scale utilizing the Synthetic Aperture Radar (SAR) imageries. This study based on intensity tracking and Differential SAR Interferometry (DInSAR) showed seasonal variations in the ice flow at the glacier tongue, and inferred that the overall interannual changes were not significant and 19% higher velocity than summer. (H. Pandit, Jawak, and Luis 2018) studied PRG to estimate velocity with Permanent Scatterer Interferometry (PS-InSAR) technique using Interferometric Wide (IW) mode Sentinel-1 Single Look Complex (SLC) images and showed average velocity approximately 400 m/a with a variation of 200 – 700 m/a from upper to lower part.

Remote sensing measurements using SAR and optical imagery are complementary in spatio temporal ice flow monitoring of glaciers. Methods involved in ice flow velocity estimation using SAR and optical imagery are offset tracking and Interferometric SAR (InSAR)/DInSAR that have been utilized widely in earlier research (Eldhuset et al. 2003; Huang and Li 2011; Zhou et al. 2014; Lemos et al. 2018; Gomez et al. 2019; Satyabala 2016; Yellala, Kumar, and Høgda 2019). Tracking the feature movement in optical imagery is limited by sun illumination, subpixel noise and cloud cover (Huang and Li 2011). Image distortion produced in optical images mainly results from subpixel noise which is generated by attitude variations (Heid and Kääb 2012; Shukla and Garg 2020). This subpixel noise generated in Landsat images used in the previous studies (Liang et al. 2019; Liu, Niu, and Yang 2018) on PRG can be eliminated by using SAR imagery with its penetration capability and ability to monitor in all-weather conditions. The choice of utilizing Sentinel-1 SAR images in the present study, hence providing reliable estimated glacier ice flow velocity. Glacier velocity estimation using InSAR/DInSAR technique due to its limitations like coherence loss, temporal decorrelation, phase noise and phase unwrapping feasibility makes offset tracking approach an alternative for glacier velocity estimation (Strozzi et al. 2002; Sangita Kumari, Ramsankaran, and Walker 2019). Offset tracking approach overcome these limitations and measure the feature movement between master and slave image using cross correlation optimization of patch intensity in the case of fast and uneven flow of glacier (Strozzi et al. 2002). Moreover, the offset tracking is more suitable for fast-moving glaciers (Sánchez-Gámez and Navarro 2017; Nela et al. 2019).

Specifically, the glacier flow velocity variations at seasonal level have been reported in West Antarctica and different mechanisms have been proposed (Nakamura, Doi, and Shibuya 2010; Zhou et al. 2014; Fahnestock et al. 2016). Seasonal acceleration at the Totten Ice Shelf has been attributed to buttressing loss from the disintegration of seasonal landfast sea ice (Greene et al. 2018). Seasonal variations in ice velocity of the Larsen B embayment showing role of summer melt percolation as well as variation of stress field in glacier dynamics (Scambos et al. 2004). On the other hand, East Antarctica gets less consideration due to its comparative stability with a slight positive mass balance.

Very few studies have been conducted to monitor specifically the PRG in East Antarctica. However, these studies reported the flow dynamics of the glacier till 2016. In this study, a remote sensing-based investigation is carried out on the PRG for the austral summer period from 2016-2019. Additionally, two months (March and April) of winter have been considered to study the changes in dynamics at the start of winter. This is undertaken by using Ground Range Detected (GRD) Interferometric Wide (IW) swath product of Sentinel-1 SAR with a detailed performance analysis of GRD product towards glacier velocity estimation in the East Antarctic region. The main objective of the present study is to estimate the recent flow velocity of the PRG through the offset tracking method, to gain insights into the dynamics of the glacier from 2016-2019.

2. Study Area and Dataset

The PRG is one of the major outlet glacier in the Prydz Bay area near Larsemann Hills and Ingrid Christensen Coast in East Antarctica (Liu, Niu, and Yang 2018; H. Pandit, Jawak, and Luis 2018). It is located at $69^{0}45''$ S and $75^{0}30''$ E (Figure 1) on Princess Elizabeth land, to the east of Amery Ice Shelf (AIS) and surrounded by Dodd Island and Meknattane Nunataks. The Indian Research Base Bharti station and Chinese Zhongshan station lie towards east at about 50 km from PRG. About 26×16 km size of enormous mass of ice detached from the glacier tongue has been reported between 1973 and 1989 (Zhou et al. 2014). The area occupied by the PRG glacier amounts to 670 sq. km (approx.), with 47 km (approx.) length from top to glacier tongue. The PRG has the narrowest width of 8 km (approx.) while the top and glacier tongue width is 25 km and 17.5 km respectively. Elevation profile of PRG varies from 16 m to 695 m respectively from glacier tongue to the upper reaches of the glacier.

Figure 1. Location of Polar Record glacier. The lines indicate the cross-sections (AB, CD, EF and GH) used for ice flow analysis.

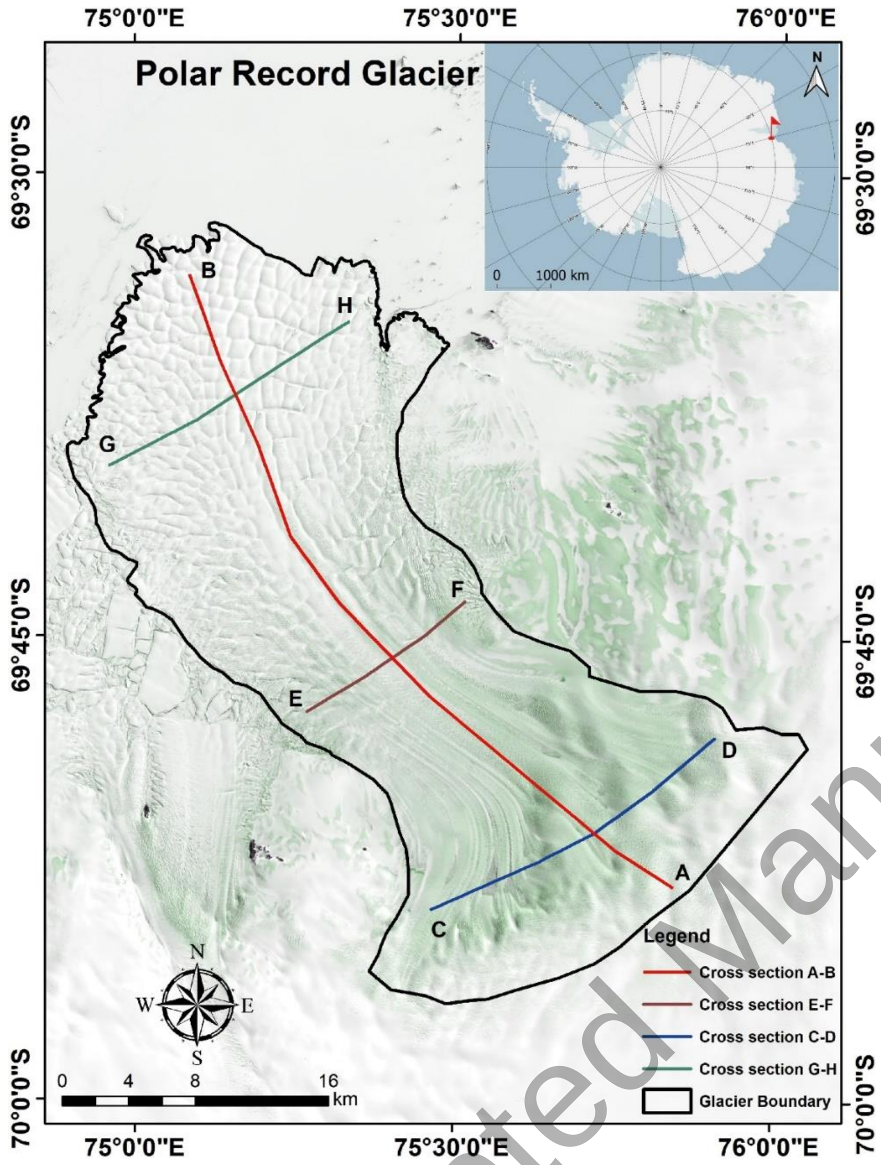

The GRD product in IW swath mode of Sentinel-1 SAR data is used in this study. This SAR data is taken from both Sentinel-1A and 1B (S1A & S1B) which was launched in April 2014 and 2016, respectively. Data comprised of C band with 5.6 cm wavelength along with a repeat cycle of 6 days interval from December to April from year 2016-2019 are taken. A total of 30 scenes (15 pairs) of single polarization with horizontal transmit and horizontal receive (HH) polarization have been utilized. Nominal resolution of S1A and S1B is 5 × 20 m (in range and azimuth direction) with an orbital phase difference of 180^0 between them. The Sentinel-1 SAR data with acquisition date are shown in Table 1.

Table 1. Sentinel-1 SAR data used in this study to estimate the glacier velocity.

S. No.	2016-2017		2017-2018		2018-2019	
	Satellite	Acquisition	Satellite	Acquisition	Satellite	Acquisition
1	S1A	17-Dec-16	S1B	18-Dec-17	S1A	19-Dec-18
2	S1B	23-Dec-16	S1A	24-Dec-17	S1B	25-Dec-18
3	S1B	16-Jan-17	S1A	17-Jan-18	S1B	18-Jan-19
4	S1A	22-Jan-17	S1B	23-Jan-18	S1A	24-Jan-19

5	S1A	15-Feb-17	S1B	16-Feb-18	S1A	17-Feb-19
6	S1B	22-Feb-17	S1A	22-Feb-18	S1B	23-Feb-19
7	S1B	17-Mar-17	S1A	18-Mar-18	S1B	19-Mar-19
8	S1A	23-Mar-17	S1B	24-Mar-18	S1A	25-Mar-19
9	S1A	16-Apr-17	S1B	17-Apr-18	S1A	18-Apr-19
10	S1B	22-Apr-17	S1A	23-Apr-18	S1B	24-Apr-19

The Reference Elevation Model of Antarctica (REMA), a high resolution Digital Elevation Model (DEM) comprised of stereoscopic DEM extracted from image pairs of 0.32 m to 0.5 m resolution. This DEM has been used as input to the ice flow velocity estimation approach. The 8 m resolution REMA terrain map may provide corrections for remote sensing based ice flow modelling. The DEM was vertically registered to Cryosat-2 and ICESat with absolute and relative uncertainties <1 m and in decimeters respectively (Howat et al. 2019). The horizontal and vertical offsets of REMA DEM scale down to the 0.2 m of DEM relative accuracy while the average accuracy of the REMA tiles are 0.6 m approximately (Howat et al. 2019). In addition to this, optical data of Landsat-8 over the period 2016-2019 have been used to demarcate the ice front position changes.

3. Methodology

3.1 Offset Tracking

The seasonal velocity is derived using SAR offset tracking which has proved as reliable technique to determine displacements using cross-correlation of the intensity image (Satyabala 2016; Luckman, Quincey, and Bevan 2007; Pritchard et al. 2005; Strozzi et al. 2002; Singh et al. 2020). This technique measures movement of glacier surface features between two images using cross-correlation optimization of patch intensity (Gray et al. 1998; Kumari, Ghosh, and Buchroithner 2014). It coregister SAR images to track offset of distinguishable features to determine glacier flow velocity (Strozzi et al. 2002). Offset tracking approach is not constrained by temporal decorrelation between pair of SAR datasets (Strozzi et al. 2002) when compared to interferometric techniques.

Overall flowchart of the method used is shown in Figure 2. This approach utilizes a selected image pair of Seninel-1 GRD product with a low temporal baseline supplied with precise orbit file for orbit correction. Image intensity affected due to additional thermal noise has been reduced by Thermal Noise Removal module provided under SNAP tool. Obtained image pair is coregistered using DEM assisted coregistration with cross-correlation to adjust the alignment from pixel of master and slave image. The approach involves cross-correlation in master and slave images using some common GCPs in these images. Using the master image GCP grid, the corresponding pixel location in slave image is located using the peak of normalized cross-correlation. The normalized cross-correlation coefficient can be estimated as equation (1) (S. Kumari, Ghosh, and Buchroithner 2014):

$$\rho(x,y) = \frac{\sum x,y(f(x,y)-f\prime)(t(x-u,y-v)-t\prime)}{\sqrt{\sum x,y(f(x,y)-f\prime)^2 \sum x,y(t(x-u,y-v)-t\prime)^2}} \quad (1)$$

Where, f' and t' are the mean of intensities in $f(x,y)$ (reference template) and $t(x-u,y-v)$ (search template) respectively. The value of coefficient lies in the range of [-1, 1].

Several window sizes (ranging from 16 × 16 to 256× 256) have been tried and the window size found to be best performing for the present study was 128*128 with pixel spacing of 40*40 (pixels), which gave the best results, were used in the present study. Unlike the existing studies for the PRG, the coregistration of image pair is performed using high resolution REMA DEM which further reduces the error (due to coregistration) in estimated glacier velocity. The peak attribute to the cross-correlation surface indicates the movement between the master and slave image (Heid and Kääb 2012).

Thus, the estimated movement is tracked in the slant and azimuth direction the range of over the glacier surface between master and slave images. The offsets computed at the GCPs give the displacement. This displacement D, can be estimated based upon the glacier movement as in equation (2):

$$D = \sqrt{\left(R_{range}\Delta x_{range}\right)^2 + (R_{azi}\Delta x_{azi})^2} \quad (2)$$

Where R_{range}, R_{azi} are pixel spacing in range and azimuth directions, and Δx_{range}, Δx_{azi} are pixel shifts in range and azimuth direction.

The displacement obtained from the GCPs utilized to estimate the velocity at these points. These velocities were interpolated on the GCP grid and finally glacier velocities for all pixels of master image were generated for the PRG. After deriving the glacier velocity, geometric correction using Range Doppler Terrain correction were applied to get the final glacier velocity maps.

Figure 2. Flowchart of the methodology used to estimate glacier velocity using offset tracking.

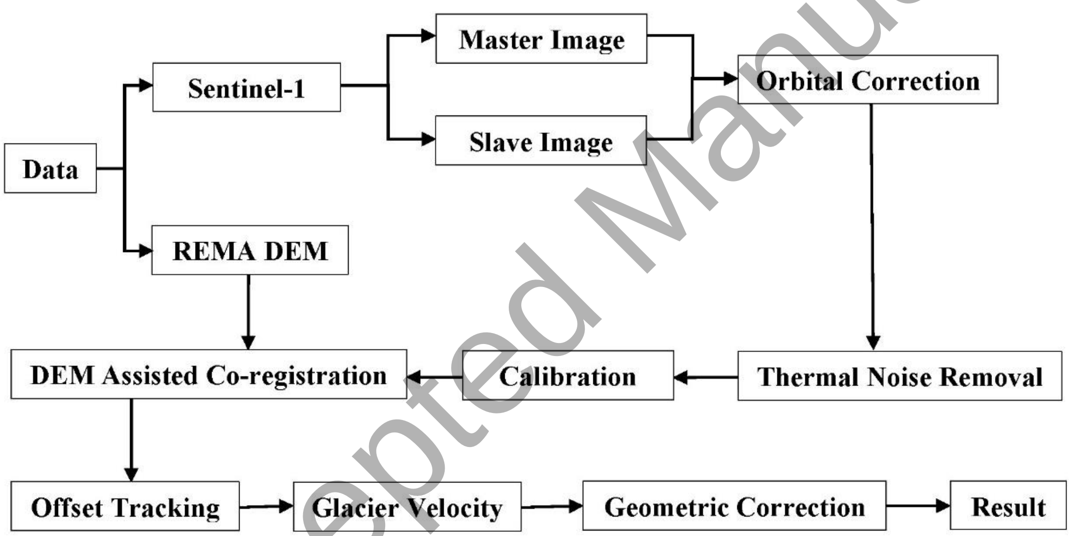

4. Results

The changes in the glacier extent, as well as annual change in the ice front position is depicted in Figure 3. The spatial distribution of ice flow velocity for PRG obtained through offset tracking is shown in Figure 4 for the period December to April (2016-2019). The ice flow direction at PRG depicted in Figure 5. Specifically, the flow along the central flow line and different cross sections spread over the glacier is shown in Figure 6 and Figure 7.

4.1 Ice front position change at the PRG

Ice front position of PRG has been changing continuously from 2004 to 2015, (Zhou et al. 2014) reported till 2012 and (Liu, Niu, and Yang 2018) reported annual frontal margin till 2015. In the present study, the changes in ice front position of PRG from 2016 to 2019 was investigated using freely available optical imagery. The Landsat-8 images acquired in austral summer were utilized to commemorate these changes in ice front position. The ice front position have been digitized manually to trace the changes in satellite imagery (Figure 3).

Figure 3. Ice front position change at Polar Record Glacier over the period of 2016-2019.

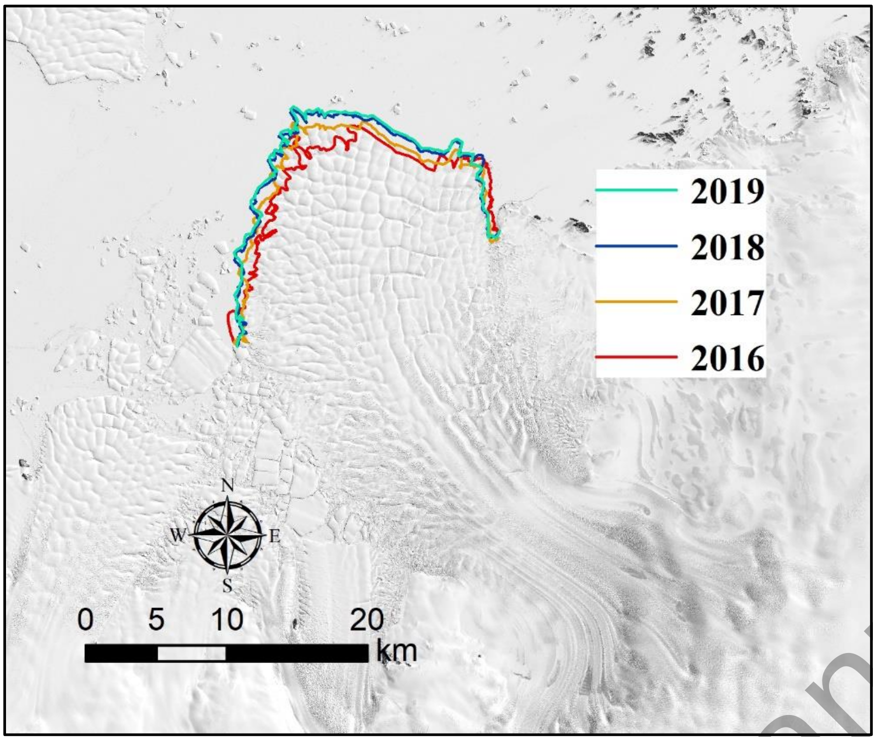

4.2 Spatial distribution of glacier velocity variations over the PRG

Seasonal velocity variations over the PRG for the period 2016-2019 in the austral summer and early winter is shown in Figure-4. Glacier flow velocity in the upper reaches is observed to be lower than the velocity in the terminus region. From 2016-2019, glacier velocity for December period demonstrates more variations in lower reaches in comparison to the variation in other months. The mean ice flow velocity has been assessed for the period of 2016-2019 and compiled in Table-2. The glacier wide mean estimated velocity for December month is varying from 1.38 m/d to 1.05 m/d. The mean glacier velocity of January month over the whole study period is showing variations from 1.62 m/d to 1.5 m/d. Similarly, the mean glacier velocity of February month varied from 1.55 m/d to 1.37 m/d. However, the mean glacier velocity of March and April showed the least variation 1.58 m/d to 1.54 m/d and 1.58 m/d to 1.56 m/d respectively. The low (negligible) variation in early winter velocity indicates a steady flow.

Table 2. Ice flow velocity of PRG for the period of 2016-2019

Period	**Mean ice flow velocity (m/d)**		
	2016-2017	**2017-2018**	**2018-2019**
December	1.38	1.35	1.05
January	1.62	1.55	1.5
February	1.55	1.56	1.37
March	1.58	1.59	1.54
April	1.58	1.56	1.56

Figure 4. Spatial distribution of PRG velocity from December to April over the period 2016-2019.

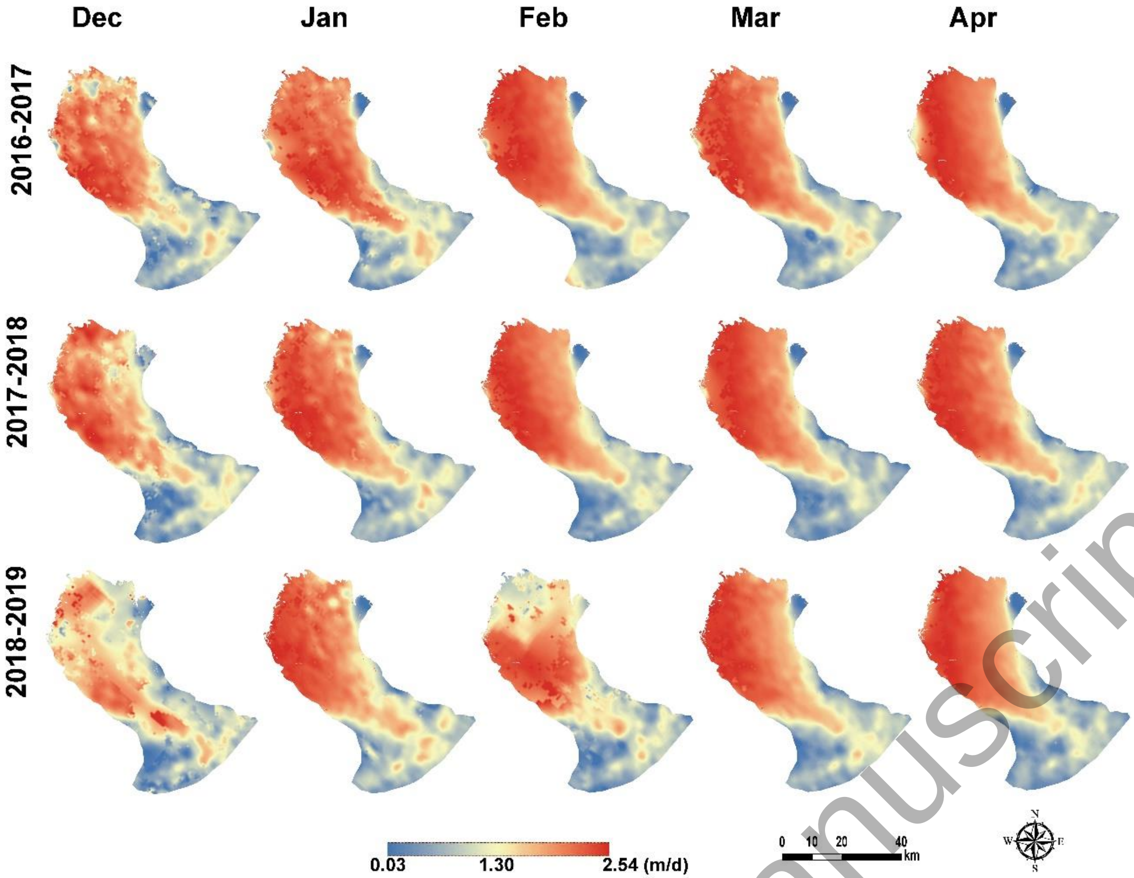

Glacier velocity in the lower reaches of 25 km (approximately) starting from glacier terminus is higher than velocity in upper reaches especially the western part of upper reaches. This low in velocity may be due to change in the course of the glacier (Figure 5) and the high velocity near the terminus can be due to the influence of the warmer temperatures near the ocean (Zhou et al. 2014). The estimated ice flow direction at PRG is depicted in Figure 5 which matches well with the reported ice flow direction by (Zhou et al. 2014).

Figure 5. Ice flow direction using Sentinel-1 (18April2019 and 24April2019) derived surface velocity vectors of PRG.

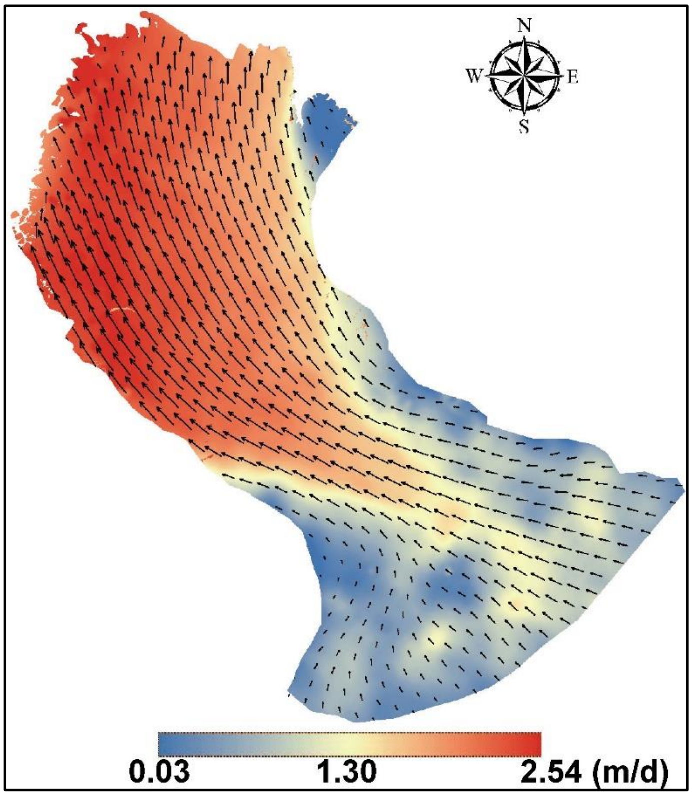

4.3 Seasonal Velocity Variations along selected Profiles

Seasonal glacier velocity variations along the profile AB (the central flowline), and other cross sectional profiles CD, EF and GH spread over the glacier extent are shown in Figure 6. Glacier velocity along the central flowline A to B (from upper reaches to lower) has been estimated monthly for the period 2016-2019 (Figure 6a-c).

Figure 6. Ice flow velocity (m/d) along cross section AB with topographic change over the period (a) 2016-2017 (b) 2017-2018 and (c) 2018-2019.

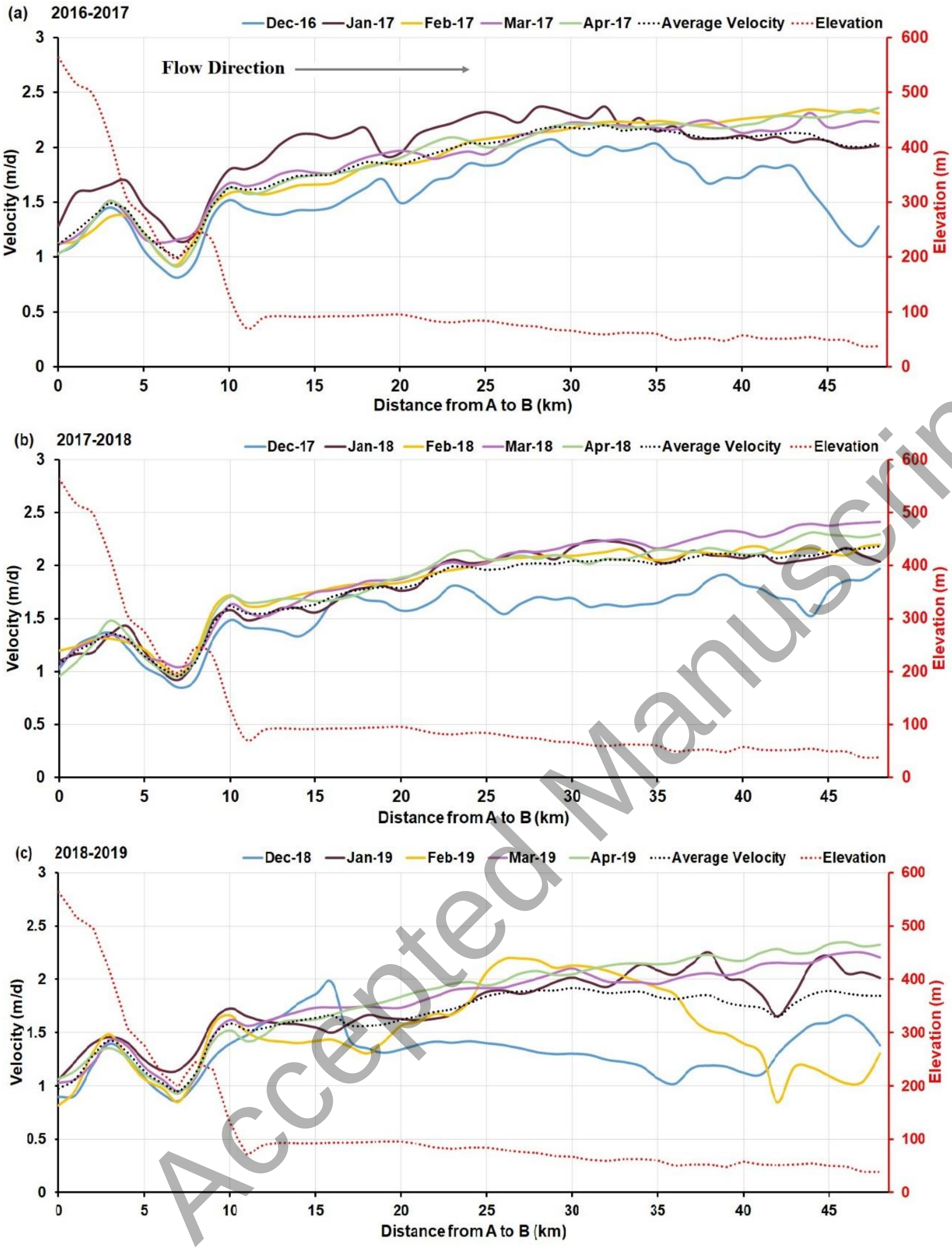

Along this profile, the ice flow velocity is found to be lower in the month of December 2016 and higher in the month of January 2017 (Figure 6a). Ice flow velocity in February, March and April (2017) is showing values close to each other i.e. showing very low change in the velocity variation. There is a dip in the glacier velocity values at distance of ~7km from A (Figure 6a-c) along with sudden change in elevation indicating the presence of grounding line of the glacier.

Similarly, for other study period 2017-2018, the glacier velocity along A to B is found lower in the month of December and highest in the month of March 2018 (Figure 6b). Similar pattern of dip in the glacier velocity (as in Figure 6a) with change in the elevation occurring in 2017-2018. For the period 2018-2019, a slight change in trend from previous period is observed. From December to February, the near terminus velocities were significantly reduced during this period. This reflected a decline in the advance of the glacier ice frontal margin (Figure 3). For April we encountered higher glacier velocity, while for December we found lower values along AB, except at the terminus region where February has the lowest velocity values. Along the central flowline, the velocity near the glacier terminus is lower in comparison to the glacier velocity at upper reaches (from A to B). Variations in the glacier velocity is more in the terminus part while upper reaches shows glacier velocity in close proximity to each month. The glacier velocity for the month of December was found to be lower than the average glacier velocity for the period of 2016-2019.

To have a detailed understanding of the flow trend over the PRG, additionally, the glacier velocity is investigated at various cross sections (shown in Figure 1) covering the whole PRG. The corresponding velocity profiles are shown in Figure 7. Cross section CD is located in the upper reaches of the glacier with a total length of ~20 km. Cross section EF lies in the middle region of the glacier having ~11.5 km of length. Cross section GH lies near the glacier terminus having the length of ~20 km. The point locations separated with a distance of 500 m on these cross sections were utilized to analyse the glacier velocities. The glacier velocity shows high variations in all month at cross section CD starting from C upto 12 km over the period 2016-2019. This variation in the glacier velocity arises due to the change in the course of glacier from upper reaches to the middle part of the glacier. More pronounced variations in the velocity values between the summer and early winter month is observed for the period of 2018-2019.

Figure 7 Ice flow velocity (m/d) over the period 2016-2019 along cross-section CD, EF and GH.

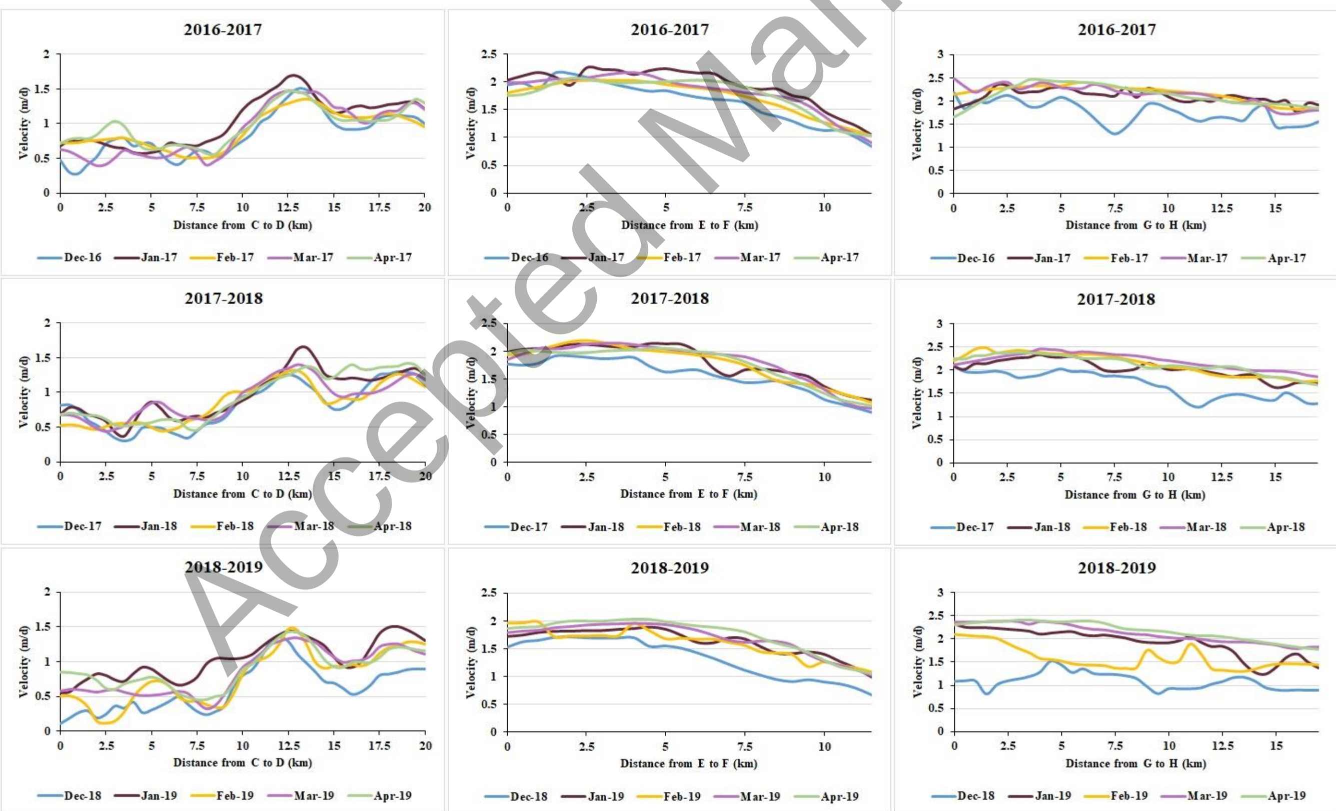

The increase in glacier velocity from 8 km to 13 km starting from C along CD cross section occurred due to relatively higher slope in the region. Also, these variations are more specifically located near C which is a point near the bending portion of the glacier. The glacier velocity in the cross section EF found to be low in December while glacier velocity for March and April are close for the period of 2016-2019. In cross section EF, 7.5 km onwards the glacier velocity is decreasing due to change in the course of flow direction. Due to the presence of cross section GH near the glacier terminus region, the glacier velocity is higher in comparison to other two upper cross sections CD and EF. The velocity profiles for all the cross sections show lowest values for December month (Figure 7). This supports our observation (Figure 4) where December month showed the least velocity.

Overall, December month consistently showcased lower glacier velocity at all the three cross sections CD, EF and GH in comparison to the glacier velocity estimated for the remaining month used in this study for analysis (Figure 7). Higher glacier velocity found in the month of March and April (2017-2019) while year 2016-2017 showing higher glacier velocity in the January month. Glacier velocity variations in March and April are following similar trend and values are nearly close.

5. Discussion

The ice front position of PRG has been reported to be varying continuously from 2004 to 2019. The average change in ice front position from 2016 to 2019 (Figure 3) was found to be ~900 m (2016-2017), ~650 m (2017-2018) and ~200 m (2018-2019). It is noted that the rate of ice front position change reported by (Liang et al. 2019) is consistent at ~600 ma^{-1} from 2004 to 2012. During 2018-2019, we found a decrease in rate of advancing in ice front position by 69% than earlier period of study (2017-2018). Ice front position has been changed with a great amount from 2016 to 2017 in comparison to the 2018-2019 where it is marginally changed. The modulation of the Ice front area led to a 25 km^2 change in glacier area from 877 km^2 to 905 km^2 over the period 2016-2019.

The glacier velocity maps generated using offset tracking have adequate spatial coverage to deliver austral summer and early winter ice speed profiles along the central flow line of PRG (Figure 4). Overall, the glacier velocity along the central flowline A-B is higher in the terminus region and lower in the upper reaches (Figure 6) during 2016-2019. Geometrical configurations of PRG have been examined to investigate the probable reasons for the heterogeneity in estimated glacier velocity (Figure 4) using surface topography from REMA DEM. It is observed from Figure 4 that the western part of the glacier is showing high velocity as well as high variations. On the other hand, glacier velocity in eastern part is low as well as less variations in the velocity values. It was also confirmed by (Zhou et al. 2014) that western part moves faster than eastern. The reason could be the difference in topography as Eastern part has higher slope than the Western part. Decline in the estimated mean glacier velocity over the period of 2016-2019 has been observed. This decline in mean glacier velocity is calculated between 2016 and 2019 and found to be 23.9%, 7.4%, 11.6%, 2.5% and 1.26% for December to April respectively. The month of early winter has least variation in decline rate. It has been suggested that least variation in glacier velocity of early winter occurred due to the start of sea ice freezing. The low (negligible) variation in early winter velocity indicates a steady flow. The decline in estimated glacier velocity from 2016 to 2019 can also be observed by change in ice front position for the same time period (Figure 3). There are several factors like sea ice, melting of ice, flow of glacier, air temperature which may affect the seasonal velocity variations of PRG (Zhou et al. 2014).

The estimated glacier velocity in austral summer is expected to be high while our study showed high velocity in early winter (Figure 4) near the glacier terminus region. The glacier terminus of PRG floating in the sea and nearby area is surrounded by sea ice. Sea ice variability near the glacier terminus of PRG from December to April over the period of 2016-2019 (Figure 8) have been analyzed for glacier velocity. It is visible in Figure 8 (a-c) that thick sea ice was present in the month of December. Changes in the sea ice condition can impact the movement of outlet glacier. The presence of thick sea ice observed during December could be the possible reason of low velocity of PRG in December month.

Figure 8. Sea ice coverage near terminus of PRG (marked in red colour) over the period of 2016-2019 for the month of December (a-c), January (d-f), February (g-i), March (j-l) and April (m) from Landsat-8 imagery.

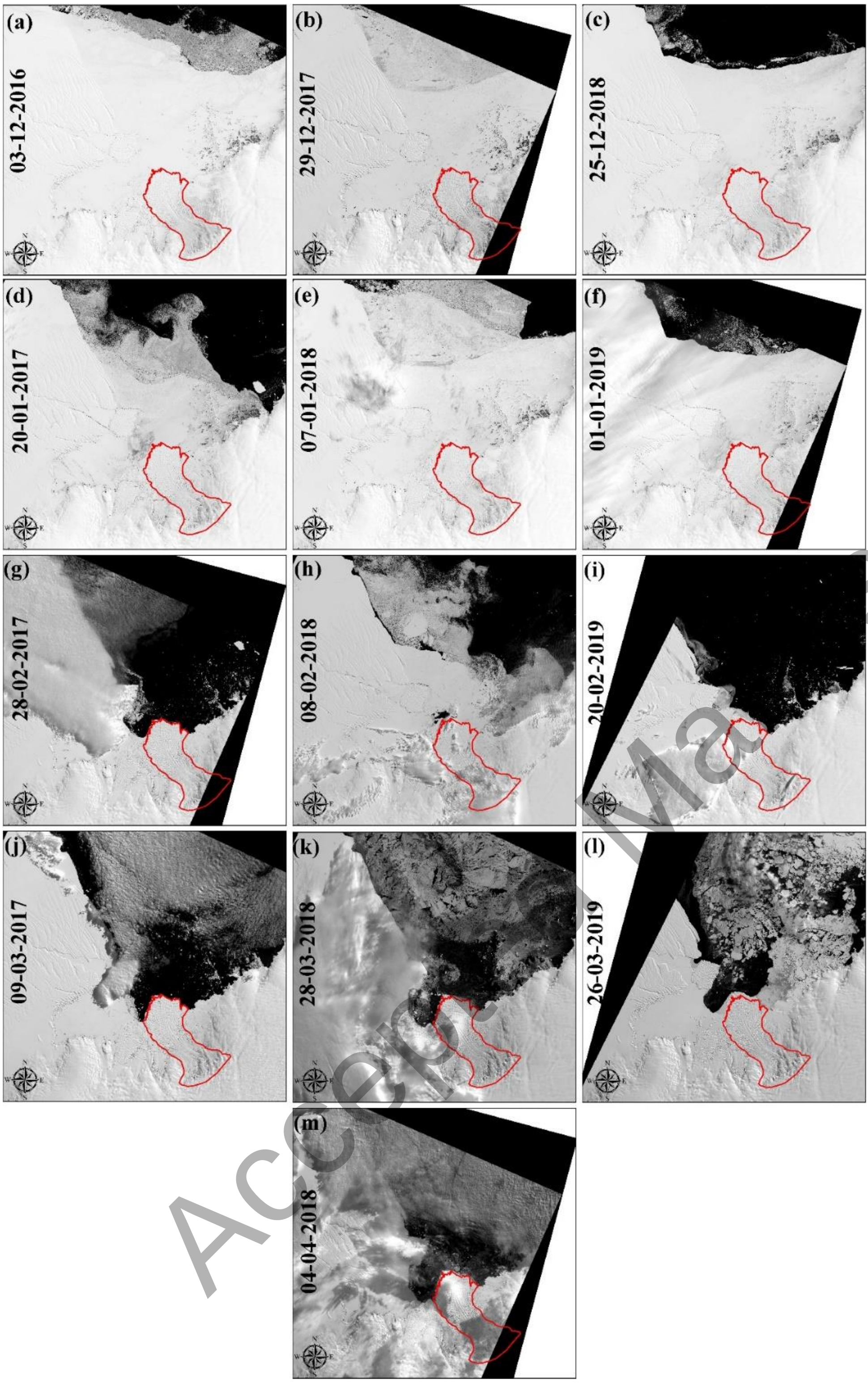

Thinning of sea ice extent was observed in January (Figure 8d-f) while PRG terminus was almost sea-ice free (Figure 8g-i) except for February 2018 (Figure 8h). From March, the sea ice started forming (Figure 8j-m) but the sea near the glacier terminus was found to be ice-free. Since cloud-free imagery (even partly obscured) for April 2017 and 2019 were not available, we analyzed only April 2018 imagery (Figure 8m). The reason for enhanced velocity in the glacier velocity map (Figure 4) in the terminus region for early winter (March and April), can be attributed to ice-free water surrounding the PRG terminus which eliminated buttressing.

We place on the record that this study provides no validation of the estimated velocity with ground truth. Field visits by the principal authors of this study have revealed that the PRG consists full of crevasses which made it difficult for helicopter landing and therefore inaccessible for the field observation. The present study follow (Shukla and Garg 2020) and (Yellala, Kumar, and Høgda 2019) for uncertainty estimation. Uncertainty in the results can occur due to the quality of satellite imagery and coregistration. Sentinel-1 SAR imagery provide cloud free and good visual contrast data to minimize errors due to poor quality images. Errors occurred due to coregistration mainly consist of low resolution DEM, this has been minimized by using high resolution REMA DEM. Errors caused by crevasse patterns, glacier deformation and glacier melting are challenging to estimate and considered here as residual error. Finally, Uncertainty estimation of the surface velocity was estimated at the stable area nearby Polar Record Glacier. The mean and standard deviation of the velocity were computed for these permanent features assuming zero movements there (Yellala, Kumar, and Høgda 2019; Shukla and Garg 2020). Uncertainty in estimated glacier ice flow velocity was found to be 0.025 m/d, by using the glacier mean velocity for all pixels at permanent features for 2016-2019. It is noted that the seasonal velocity estimated for PRG for 2016-2019 is quite variable which is in agreement with the findings of earlier studies on PRG (Liang et al. 2019; Zhou et al. 2014; Liu, Niu, and Yang 2018).

This study reports the glacier velocity >2 m/d for some parts over the period 2016-2019, which was also reported by (Zhou et al. 2014). This study focuses the glacier velocity estimation in austral summer and early winter as prime movement on glacier surface occur only in this season (Liang et al. 2019; Zhou et al. 2014; Liu, Niu, and Yang 2018). Changes in the glacier tongue speed extends ~25 km from the glacier terminus in the present study, similar to the (Liang et al. 2019) while (Zhou et al. 2014) reported these changes extends ~15 km from glacier terminus. The seasonal glacier velocity estimated for PRG over the period of 2016-2019 are quite variable, in agreement with the outcomes of earlier studies (Liang et al. 2019; Zhou et al. 2014; Liu, Niu, and Yang 2018) based on PRG.

6. Summary and Conclusions

This study focuses on recent seasonal (austral summer and early winter) variation of ice velocity for PRG from 2016 to 2019, which was computed by using an offset tracking approach applied to GRD product of Sentinel-1 image pairs. The present study extends earlier analyses of glacier velocity change at PRG (Zhou et al. 2014; Liang et al. 2019; Liu, Niu, and Yang 2018). The adoption of Sentinel-1 data improves upon results derived from optical sensors and DInSAR based results for glacier velocity due to its low temporal baseline, high resolution, and 16-bit radiometric resolution. This leads to better estimates of seasonal velocity variations and reduced errors. To further reduce the error due to coregistraion, the high resolution REMA DEM was used in the study to estimate glacier velocity.

Significant findings of this study are as follows. The average ice front position receded from ~900 m in 2016-2017 to ~650 m in 2017-2018 to ~200 m in 2018-2019. However, a slowdown near the glacier terminus is observed for the period 2018-2019, which led to the glacier advance by 25-km^2 from 877 km^2 to 905 km^2. The enhanced velocity at the terminus in the early winter (March and April) was attributed to ice-free water surrounding the PRG terminus which eliminated the buttressing. Through this investigation, it is found that there was no significant change in the velocity of the PRG, both in spatial and temporal domains. Moreover, the ice velocities at PRG have varied seasonally (Liang et al. 2019). We will continue to monitor the PRG over an extended time frame and report significant changes if any.

Acknowledgements

We gratefully acknowledge the Director, National Centre for Polar and Ocean Research, Ministry of Earth Sciences, for motivation. Sentinel-1 data were provided by the European Space Agency in the public domain. The high-resolution REMA DEM was provided by the University of Minnesota. We also thank USGS for providing Landsat-8 data in the public domain.

References:

Bindschadler, R., H. Choi, A. Wichlacz, R. Bingham, J. Bohlander, K. Brunt, H. Corr, et al. 2011. “Getting around Antarctica: New High-Resolution Mappings of the Grounded and Freely-Floating Boundaries of the Antarctic Ice Sheet Created for the International Polar Year.” *Cryosphere* 5 (3): 569–88. doi:10.5194/tc-5-569-2011.

Eldhuset, K., P. H. Andersen, S. Hauge, E. Isaksson, and D. J. Weydahl. 2003. “ERS Tandem InSAR Processing for DEM Generation, Glacier Motion Estimation and Coherence Analysis on Svalbard.” *International Journal of Remote Sensing* 24 (7): 1415–37. doi:10.1080/01431160210153039.

Fahnestock, Mark, Ted Scambos, Twila Moon, Alex Gardner, Terry Haran, and Marin Klinger. 2016. “Rapid Large-Area Mapping of Ice Flow Using Landsat 8.” *Remote Sensing of Environment* 185. The Authors: 84–94. doi:10.1016/j.rse.2015.11.023.

Gomez, Rodrigo, Jorge Arigony-Neto, Angela De Santis, Saurabh Vijay, Ricardo Jaña, and Andres Rivera. 2019. “Ice Dynamics of Union Glacier from SAR Offset Tracking.” *Global and Planetary Change* 174 (December 2018). Elsevier: 1–15. doi:10.1016/j.gloplacha.2018.12.012.

Gray, A. L., K. E. Mattar, P. W. Vachon, R. Bindschadler, K. C. Jezek, R. Forster, and J. P. Crawford. 1998. “InSAR Results from the RADARSAT Antarctic Mapping Mission Data: Estimation of Glacier Motion Using a Simple Registration Procedure.” *International Geoscience and Remote Sensing Symposium (IGARSS)* 3 (1): 1638–40. doi:10.1109/igarss.1998.691662.

Greene, Chad A., Duncan A. Young, David E. Gwyther, Benjamin K. Galton-Fenzi, and Donald D. Blankenship. 2018. “Seasonal Dynamics of Totten Ice Shelf Controlled by Sea Ice Buttressing.” *Cryosphere* 12 (9): 2869–82. doi:10.5194/tc-12-2869-2018.

H. Pandit, Prashant, Shridhar D. Jawak, and Alvarinho J. Luis. 2018. “Estimation of Velocity of the Polar Record Glacier, Antarctica Using Synthetic Aperture Radar (SAR).” *Proceedings* 2 (7): 332. doi:10.3390/ecrs-2-05145.

Hanna, Edward, Francisco J. Navarro, Frank Pattyn, Catia M. Domingues, Xavier Fettweis, Erik R. Ivins, Robert J. Nicholls, et al. 2013. “Ice-Sheet Mass Balance and Climate Change.” *Nature*

498 (7452). Nature Publishing Group: 51–59. doi:10.1038/nature12238.

Heid, T., and A. Kääb. 2012. “Evaluation of Existing Image Matching Methods for Deriving Glacier Surface Displacements Globally from Optical Satellite Imagery.” *Remote Sensing of Environment* 118. Elsevier Inc.: 339–55. doi:10.1016/j.rse.2011.11.024.

Howat, Ian M., Claire Porter, Benjamin E. Smith, Myoung Jong Noh, and Paul Morin. 2019. “The Reference Elevation Model of Antarctica.” *Cryosphere* 13 (2): 665–74. doi:10.5194/tc-13-665-2019.

Huang, Lei, and Zhen Li. 2011. “Comparison of SAR and Optical Data in Deriving Glacier Velocity with Feature Tracking.” *International Journal of Remote Sensing* 32 (10): 2681–98. doi:10.1080/01431161003720395.

Kumari, S., S. K. Ghosh, and M. F. Buchroithner. 2014. “Measurement of Glacier Velocity at Pik Lenin, Tajikistan, by Feature Tracking.” *International Archives of the Photogrammetry, Remote Sensing and Spatial Information Sciences - ISPRS Archives* 40 (8): 531–36. doi:10.5194/isprsarchives-XL-8-531-2014.

Kumari, Sangita, Raaj Ramsankaran, and Jeffrey P. Walker. 2019. “Impact of Window Size in Remote Sensing Based Glacier Feature Tracking - A Study on Chhota Shigri Glacier, Western Himalayas, India.” *International Geoscience and Remote Sensing Symposium (IGARSS)*, no. December 2020: 4175–78. doi:10.1109/IGARSS.2019.8899325.

Lemos, Adriano, Andrew Shepherd, Malcolm McMillan, and Anna E. Hogg. 2018. “Seasonal Variations in the Flow of Land-Terminating Glaciers in Central-West Greenland Using Sentinel-1 Imagery.” *Remote Sensing* 10 (12): 1–12. doi:10.3390/rs10121878.

Liang, Q. I., Chunxia Zhou, Ian A.N.M. Howat, Seongsu Jeong, Ruixi Liu, and Yiming Chen. 2019. “Ice Flow Variations at Polar Record Glacier, East Antarctica.” *Journal of Glaciology* 65 (250): 279–87. doi:10.1017/jog.2019.6.

Liu, Tingting, Muye Niu, and Yuande Yang. 2018. “Ice Velocity Variations of the Polar Record Glacier (East Antarctica) Using a Rotation-Invariant Feature-Tracking Approach.” *Remote Sensing* 10 (1). doi:10.3390/rs10010042.

Luckman, Adrian, Duncan Quincey, and Suzanne Bevan. 2007. “The Potential of Satellite Radar Interferometry and Feature Tracking for Monitoring Flow Rates of Himalayan Glaciers.” *Remote Sensing of Environment* 111 (2): 172–81. doi:10.1016/j.rse.2007.05.019.

Nakamura, Kazuki, Koichiro Doi, and Kazuo Shibuya. 2010. “Fluctuations in the Flow Velocity of the Antarctic Shirase Glacier over an 11-Year Period.” *Polar Science* 4 (3). Elsevier B.V. and

NIPR: 443–55. doi:10.1016/j.polar.2010.04.010.

Nela, Bala Raju, Debmita Bandyopadhyay, Gulab Singh, Andrey F. Glazovsky, Ivan I. Lavrentiev, Tatiana E. Kromova, and Jorge Arigony-Neto. 2019. "Glacier Flow Dynamics of the Severnaya Zemlya Archipelago in Russian High Arctic Using the Differential Sar Interferometry (DInSAR) Technique." *Water (Switzerland)* 11 (12). doi:10.3390/w11122466.

Pritchard, Hamish, Tavi Murray, Adrian Luckman, Tazio Strozzi, and Stuart Barr. 2005. "Glacier Surge Dynamics of Sortebræ, East Greenland, from Synthetic Aperture Radar Feature Tracking." *Journal of Geophysical Research: Earth Surface* 110 (3): 1–13. doi:10.1029/2004JF000233.

Raup, Bruce H., Liss M. Andreassen, Tobias Bolch, and Suzanne Bevan. 2014. *Remote Sensing of Glaciers*. *Remote Sensing of the Cryosphere*. doi:10.1002/9781118368909.ch7.

Rémy, Frédérique, and Massimo Frezzotti. 2006. "Antarctica Ice Sheet Mass Balance." *Comptes Rendus - Geoscience* 338 (14–15): 1084–97. doi:10.1016/j.crte.2006.05.009.

Rignot, E., S. Jacobs, J. Mouginot, and B. Scheuchl. 2013. "Ice-Shelf Melting around Antarctica." *Science* 341 (6143): 266–70. doi:10.1126/science.1235798.

Rignot, Eric. 2002. "Mass Balance of East Antarctic Glaciers and Ice Shelves from Satellite Data." *Annals of Glaciology* 34: 217–27. doi:10.3189/172756402781817419.

Sahu, Rakesh, and R. D. Gupta. 2019. "Spatiotemporal Variation in Surface Velocity in Chandra Basin Glacier between 1999 and 2017 Using Landsat-7 and Landsat-8 Imagery." *Geocarto International*. Taylor & Francis: 1–21. doi:10.1080/10106049.2019.1659423.

Sánchez-Gámez, Pablo, and Francisco J. Navarro. 2017. "Glacier Surface Velocity Retrieval Using D-InSAR and Offset Tracking Techniques Applied to Ascending and Descending Passes of Sentinel-1 Data for Southern Ellesmere Ice Caps, Canadian Arctic." *Remote Sensing* 9 (5): 1–17. doi:10.3390/rs9050442.

Satyabala, S. P. 2016. "Spatiotemporal Variations in Surface Velocity of the Gangotri Glacier, Garhwal Himalaya, India: Study Using Synthetic Aperture Radar Data." *Remote Sensing of Environment* 181. Elsevier Inc.: 151–61. doi:10.1016/j.rse.2016.03.042.

Scambos, T. A., J. A. Bohlander, C. A. Shuman, and P. Skvarca. 2004. "Glacier Acceleration and Thinning after Ice Shelf Collapse in the Larsen B Embayment, Antarctica." *Geophysical Research Letters* 31 (18): 2001–4. doi:10.1029/2004GL020670.

Shukla, Aparna, and Purushottam Kumar Garg. 2020. "Spatio-Temporal Trends in the Surface Ice Velocities of the Central Himalayan Glaciers, India." *Global and Planetary Change* 190

(August 2019). Elsevier: 103187. doi:10.1016/j.gloplacha.2020.103187.

Singh, Gulab, Bala Raju Nela, Debmita Bandyopadhyay, Shradha Mohanty, and Anil V. Kulkarni. 2020. “Discovering Anomalous Dynamics and Disintegrating Behaviour in Glaciers of Chandra-Bhaga Sub-Basins, Part of Western Himalaya Using DInSAR.” *Remote Sensing of Environment* 246 (October 2019). Elsevier: 111885. doi:10.1016/j.rse.2020.111885.

Stearns, Leigh A. 2011. “Dynamics and Mass Balance of Four Large East Antarctic Outlet Glaciers.” *Annals of Glaciology* 52 (59): 116–26. doi:10.3189/172756411799096187.

Stearns, Leigh A., Benjamin E. Smith, and Gordon S. Hamilton. 2008. “Increased Flow Speed on a Large East Antarctic Outlet Glacier Caused by Subglacial Floods.” *Nature Geoscience* 1 (12): 827–31. doi:10.1038/ngeo356.

Strozzi, Tazio, Adrian Luckman, Tavi Murray, Urs Wegmüller, and Charles L. Werner. 2002. “Glacier Motion Estimation Using SAR Offset-Tracking Procedures.” *IEEE Transactions on Geoscience and Remote Sensing* 40 (11): 2384–91. doi:10.1109/TGRS.2002.805079.

Yellala, Abhilash, Vijay Kumar, and Kjell Arild Høgda. 2019. “Bara Shigri and Chhota Shigri Glacier Velocity Estimation in Western Himalaya Using Sentinel-1 SAR Data.” *International Journal of Remote Sensing* 40 (15). Taylor & Francis: 5861–74. doi:10.1080/01431161.2019.1584685.

Zhou, Chunxia, Yu Zhou, Fanghui Deng, Songtao Ai, Zemin Wang, and E. Dongchen. 2014. “Seasonal and Interannual Ice Velocity Changes of Polar Record Glacier, East Antarctica.” *Annals of Glaciology* 55 (66): 45–51. doi:10.3189/2014AoG66A185.